Electrochemical and Solid-State Letters, **2** (4) 157-160 (1999)
S1099-0062(98)11-078-7 CCC: $7.00 © The Electrochemical Society, Inc.

In Situ Synchrotron X-Ray Diffraction Studies of the Phase Transitions in $Li_xMn_2O_4$ Cathode Materials

X. Q. Yang,[a,*,z] X. Sun,[a] S. J. Lee,[a] J. McBreen,[a,*] S. Mukerjee,[b,*] M. L. Daroux,[c,*] and X. K. Xing[c,*]

[a]*Brookhaven National Laboratory, Upton, New York 11973, USA*
[b]*Department of Chemistry, Northeastern University, Boston, Massachusetts 02115-5000, USA*
[c]*Gould Electronics Incorporated, Eastlake, Ohio 44095-4001, USA*

In situ X-ray diffraction studies of $Li_xMn_2O_4$ spinel cathode materials during charge-discharge cycling were carried out using a synchrotron as the X-ray source. Lithium-rich (x = 1.03-1.06) spinel materials, obtained from two different sources, were studied. Three cubic phases with different lattice constants were observed during charge-discharge cycles in all of the samples when a sufficiently low charge-discharge rate (≤C/10) was used. There were two regions of two-phase coexistence, which indicates that both phase transitions are first order. The separation of the Bragg peaks representing these three phases varied from sample to sample and also depended on the charge-discharge rate. These results show that the deintercalation of lithium in lithium-rich spinel cathode materials proceeds through a series of phase transitions from a lithium-rich phase to a lithium-poor phase and finally to a λ-MnO_2-like cubic phase, rather than through a continuous lattice constant contraction in a single phase.

Manuscript received November 25, 1998. Available electronically January 25, 1999.

The $Li_xMn_2O_4$ spinel is one of the most promising cathode materials for lithium rechargeable batteries because of its low cost and low toxicity. Recent studies have focused on the problem of capacity fading of this material during cycling, especially at elevated temperature. This fading has been attributed to two sources, the dissolution of Mn^{2+} into the nonaqueous electrolytes[1] and the inhomogeneity of the spinel local structure.[2,3] Early ex situ X-ray diffraction studies of $Li_xMn_2O_4$ were performed by Ohzuku et al.[4] They found that two cubic phases coexist for $0.60 > x > 0.27$, and a single cubic phase is present for $1.0 > x > 0.6$. Xia and Yoshio[5] reported in their studies that the two-phase coexistence was suppressed in cathode materials which were prepared lithium rich (x = 1.04) or oxygen rich. They also claimed that the two-phase coexistence is one of the key factors for the capacity fading during cycling. By suppressing this phase transition, the capacity fading of the lithium-rich cathode materials was significantly improved at the expense of lower initial capacity. In their later X-ray diffraction (XRD) studies,[6] an in situ technique was used, and the same conclusion that there was a one-phase structure for lithium-rich spinel was presented. This interesting work raised an important issue: the relationship between the structural change and the capacity fading of these spinel materials during cycling. However, there are experimental data published by other research groups that show two-phase coexistence in lithium-rich spinels. For example, Richard et al.[7] have reported their in situ XRD studies with the observation of two-phase coexistence in the $0.60 > x > 0.27$ range for $Li_xMn_2O_4$ material, where the x value before charge was similar to that in the studies of Ref. 5 (x = 1.02 vs. x = 1.04). The main difference between these two studies is the charge rate (C/40 in Ref. 7 vs. C/3 in Ref. 5). The first issue to address in this article is whether the two-phase coexistence region is being suppressed in a lithium-rich spinel. The second issue is whether the spinel is a two-phase or a three-phase system during lithium deintercalation and the determination of the order of the phase transitions. This issue was raised recetnly when Liu et al.[8] published in situ XRD and neutron diffraction studies for spinel materials. A new phase diagram for $Li_xMn_2O_4$ during discharge was proposed: from single-phase A ($0 < x < 0.2$) to a two-phase coexistence region A+B ($0.2 < x < 0.4$), to a single-phase B ($0.45 < x < 0.55$), and finally to a single-phase C ($0.55 < x < 1$). This three-phase model is interesting and different from the two-phase system proposed by Ohzuku in Ref. 4. Because no two-phase coexistence region was observed between phase B and phase C in Liu's study, they claim that the phase transition between B and C is second order. In this paper, experimental evidence is presented for the first time to show that the three-phase model is correct but that both phase transitions are first order. The unique technique used in this in situ study was the utilization of the synchrotron radiation as the X-ray source. By using this technique, we were able to probe the cathode bulk in a transmission mode. Therefore, more detailed structural changes during lithium deintercalation and intercalation were observed. The effects of charge-discharge rate on the structural change behavior of these spinel materials are also discussed.

Experimental

Sample A, $Li_xMn_2O_4$ (x = 1.05) powder, was obtained from Gould Electronics Inc., and sample B, $Li_xMn_2O_4$ (x = 1.03-1.06) powder, was purchased from EM Industries Inc. Cathodes were prepared by slurrying $Li_xMn_2O_4$ powder with 10% poly(vinylidene dichloride) (KynarFlex 2801, Atochem) and 10% acetylene black (w/w) in a fugitive solvent, then coating the mix onto Al foil. After vacuum drying at 100°C, the electrode disks (2.8 cm^2) were punched and weighed. The average weight of active material was 20 mg. The electrodes were incorporated into cells with a Li foil negative electrode, a Celgard separator, and a 1 M $LiPF_6$ electrolyte in a 1:1:3 propylene carbonate:ethylene carbonate:dimethyl carbonate solvent (LP 10 from EM Industries Inc.). Mylar windows instead of beryllium windows were used in these in situ cells.

In situ XRD spectra were collected on beam line X18A at the National Synchrotron Light Source at Brookhaven National Laboratory operated at an energy of 10375 eV (λ =1.195 Å). The experimental setup was basically the same as described in our previous paper.[9] The battery cells were charged continuously during XRD data collection.

Results and Discussion

Figure 1 shows the in situ XRD spectra of sample A during the first charge from 3.5 to 4.5 V under constant-current conditions at the C/6 rate. The x value was assigned to each scan based on the assumption that the x value decreased uniformly from 1.05 to 0 during the charging process. The missing data toward the end of charge was due to the unavailability of the X-ray beam. Because the charging process was continued during this period, the incomplete data were included in the plot to provide a correct indication of the progression of charge states. All in situ spectra in this paper are treated in the same way. Because the cubic structure of the $Li_xMn_2O_4$ spinel is well known (space group *Fd*3*m*), only three Bragg peaks, (511), (440), and (531), were recorded for each 2θ scan (32 min for each scan). From the spectra in Fig. 1, only one cubic phase can be clearly identified with all three peaks moving to higher angles in a continuous fashion during charge. The calculated lattice constant of the cubic unit cell, based on the position of (531) peak, contracted from 8.25 Å for the uncharged cell to 8.07 Å for the fully charged cell. (As

* Electrochemical Society Active Member.
z E-mail: XYANG@BNL.GOV

S1099-0062(98)11-078-7 CCC: $7.00

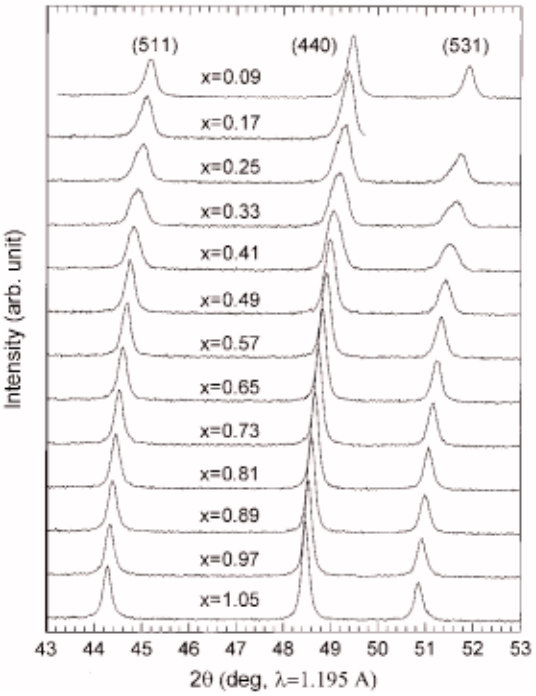

Figure 1. In situ XRD patterns of $Li_xMn_2O_4$ sample A during first charge at a C/6 rate, 32 min for each scan.

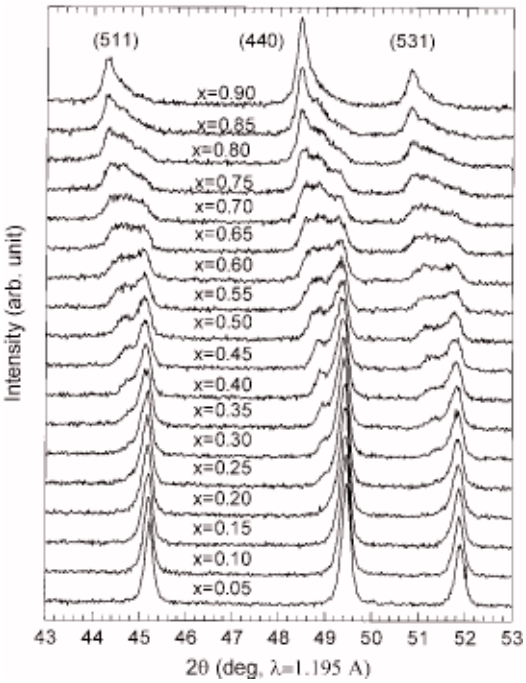

Figure 2. In situ XRD patterns of $Li_xMn_2O_4$ sample A during first discharge at a C/6 rate, 16 min for each scan.

the calculation is based on one peak only, the error in lattice constants is in the range of 0.02 Å.) This is in good agreement with the results reported by Xia and Yoshio.[5,6] However, because a slower charge rate (C/6 vs. C/3) and an in situ technique were used here, more detailed structural changes were recorded in Fig. 1. All three peaks began to broaden when the cell was charged to $x = 0.41$, and became narrower at $x = 0.09$. This is an indication of a two-phase coexistence and a phase transition in this region. In order to record more spectra during discharge, the data collection time for each 2θ scan was reduced from 32 to 16 min while the discharge rate was held at the same C/6 rate. The results are plotted in Fig. 2. Although the signal-to-noise ratio of the spectra was not as good as in Fig. 1 due to the shorter data collecting time, clear phase transitions were observed through the spectra in Fig. 2. During discharge, starting from $x = 0.20$, a set of new peaks appeared at lower angles and grew in intensity at the expense of the intensity of the original peaks. At $x = 0.60$, the third set of peaks emerged and finally became the dominant peaks at the end of discharge. It is clear from the spectra in Fig. 2 that the cathode material went through distinguishable cubic phases during discharge. However, from scan $x = 0.30$ to 0.85, all the Bragg peaks are broad and not well resolved, indicating the nonequilibrium state of the system.

We then decided to study this sample with a slower charge-discharge rate. To eliminate any unpredictable factors introduced by the cycling history of the first cell, a fresh cell was constructed for the slower charge-discharge rate studies. The cathode disk used in the second cell was punched from the same batch as the first cell. The charge rate was reduced from C/6 to C/10, and the data collecting time was 32 min for each 2θ scan. The spectra are plotted in Fig. 3. All three phases observed in Fig. 2 are clearly resolved in Fig. 3. At $x = 0.90$, all three peaks begin growing broader. With decreasing values of x, the width of the three peaks continues to increase. Clear peak separation can be observed in scans at $x = 0.60$ and 0.55. The new peaks representing the third phase emerged in the scan at $x = 0.40$. They became the dominating peaks at the end of charge in the scan at $x = 0.05$. For this lithium-rich spinel cathode material (sample A), three cubic phases with different lattice constants can be clearly identified during charge. We refer to them as phase I, phase II, and phase III. Unlike the clear peak separation in scans with $x = 0.20$ and 0.15, the peak separation in scans with $x = 0.55$ and 0.50 is small and could easily be missed if the charge rate is too high. Figure

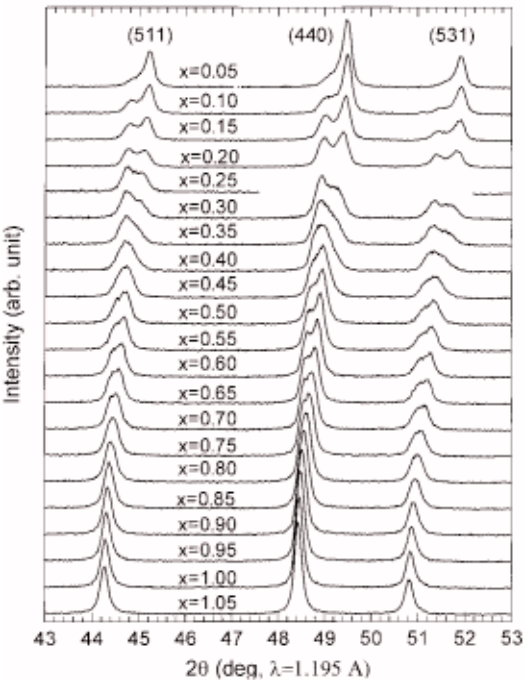

Figure 3. In situ XRD patterns of $Li_xMn_2O_4$ sample A during first charge at a C/10 rate, 32 min for each scan.

4 is a plot of the charging curve of this cell with a slower (C/10) rate. This is a typical charging curve for the $Li_xMn_2O_4$ spinel with two plateaus. This curve was divided into five regions based on the two plateaus. From $x = 1.05$ to 0.95, the curve is a steep slope, this region is assigned to a single phase I. From $x = 0.95$ to 0.55, the first plateau at ~4.05 V is attributed to a phase I + phase II coexistence region. From $x = 0.55$ to 0.44, the curve is the step between the two plateaus, this region is assigned to a single phase II. From $x = 0.44$ to 0.06, the second plateau at ~4.15 V is attributed to the phase II + phase III coexistence region. From $x = 0.06$ to 0, the steep slope region is assigned to a single phase III. Comparing the phase diagram based on the shape of the charging curve in Fig. 4 and the phase separation observed in Fig. 3, the I + II region and II + III region matched well

S1099-0062(98)11-078-7 CCC: $7.00

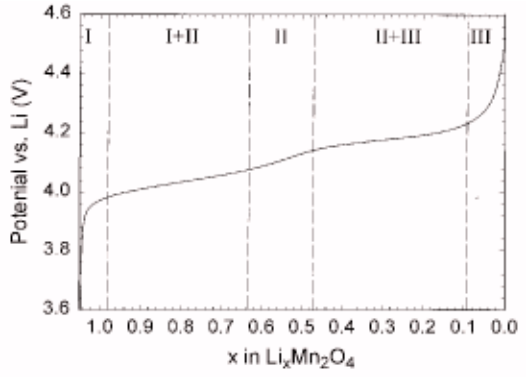

Figure 4. The first charge curve of the $Li/Li_xMn_2O_4$ cell, using sample A as cathode, at a C/10 rate.

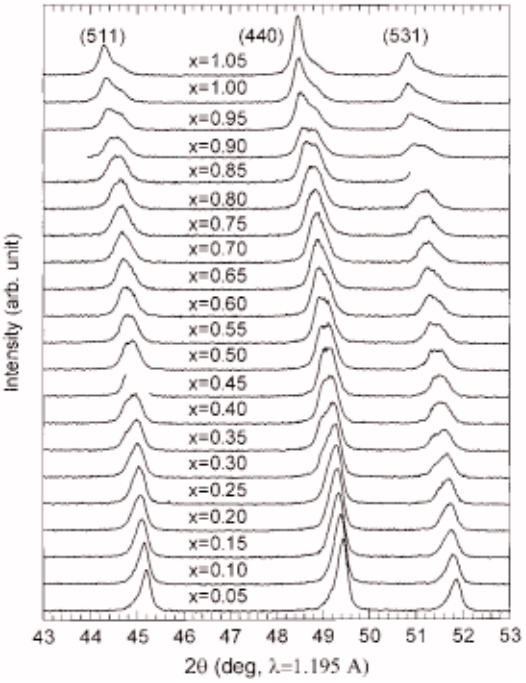

Figure 5. In situ XRD patterns of $Li_xMn_2O_4$ sample A during first discharge at a C/10 rate, 32 min for each scan.

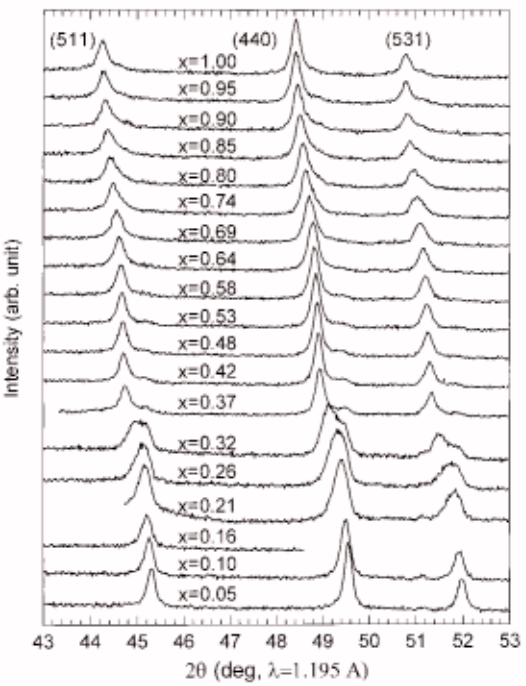

Figure 6. In situ XRD patterns of $Li_xMn_2O_4$ sample B during first discharge at a C/10 rate, 32 min for each scan.

with the XRD spectra in Fig. 3. However, from $x = 0.55$ to 0.4, rather than observing the single phase II as expected, both phase I and phase II are observed in Fig. 3. This inconsistency between the XRD data and the charging curve is due to the nonequilibrium state of the system caused by the fast charging rate. This retardation effect is more pronounced in Fig. 2 where the rate is even faster. The voltage measured in the charging curve is determined by the composition of cathode at the electrolyte-cathode interface, which can be quite different from the bulk when the charging rate is high. The XRD spectra during discharge (C/10 rate) for the same cell are plotted in Fig. 5. The data collection time for each 2θ scan is 32 min. The reversible transitions from phase III to phase II and then from phase II to phase I are confirmed. However, the peak separation is not as clear as in Fig. 3 for charging.

$Li_xMn_2O_4$ spinel samples obtained from other commercial sources such as Sedema Division of Sadacem and EM Industries Inc. were also studied. All of them showed the same three-phase behavior during charge-discharge cycles if a sufficiently slow charge-discharge rate was used. Due to the limited length of this paper, we present here only the results for sample B (EM Industries Inc.). This sample is also a lithium-rich $Li_xMn_2O_4$ ($x = 1.03$-1.06) spinel material. The results of samples from other sources will be discussed in later publications. The in situ XRD spectra of sample B during the first discharge are plotted in Fig. 6. The data collection time was 32 min for each 2θ scan and the discharge rate was C/10. All three phases observed in Fig. 5 can be identified in Fig. 6. Clear peak separations are observed at $x = 0.32$ in the phase III and phase II coexistence region. On the other hand, the phase II and phase I coexistence region is recognizable through the peak broadening, but no clear peak separations are observed.

As discussed in the introduction, one important issue we want to address in this paper is the structural change behavior of the lithium-rich samples. For this purpose, both samples A and B used in this study are lithium rich. As demonstrated by the spectra in Fig. 1, when a fast charge rate was used, the phase transitions were masked. As the charging rate used in Ref. 5 was even faster (C/3), it may have masked the phase transition and led the authors to conclude that the phase transition was suppressed in lithium-rich samples. However, when slower charge rates were used in this study, clear phase transitions were observed in our lithium-rich samples. Also, when the same rate was used for both charge and discharge, the peak separations in Fig. 3 for charge are much clearer than in Fig. 5 for discharge. This tells us that many other factors, such as the electrochemical history of the cell, the nucleation of the new crystal phase, and the original crystal grain size of the samples, have significant effects on the XRD spectra. Based on our results on lithium-rich samples obtained from two different sources, we believe that the phase transitions are not suppressed in lithium-rich samples. Therefore, the relationship between the capacity fading and the phase transitions also must be reevaluated.

The phase diagram of the $Li_xMn_2O_4$ spinel material in Fig. 4 derived from the in situ XRD spectra, is different from the two-phase model. The two-phase model was first proposed by Ohzuku et al.[4] and widely accepted by most research groups in this field. The three-phase model was first proposed by Liu et al.[8] However, the ex situ XRD technique used in Ref. 8 was not able to resolve the two-phase coexistence region between phase I and phase II (phases C and B in Ref. 8). Therefore, this transition was mistakenly assigned as a second-order phase transition and the two-phase coexistence region was mistakenly assigned as single-phase C. From Fig. 2, 3, 5, and 6, a clear two-phase coexistence region of phase I and phase II was observed. Therefore, we conclude that the transition between them was a first-order phase transition. The three-phase model presented here is also in good agreement with the results of cyclic voltammetry studies[10] which concluded that a two-step deintercalation process was responsible for the two oxidation peaks during charge. Although the phase I to phase II transition and the two-phase coexistence region have not been recognized, their existence was hinted at in several published papers. For example, a small discontinuous gap of

S1099-0062(98)11-078-7 CCC: $7.00

ca. 0.02 Å is observed around $x = 0.55$ in Ref. 5. The same gap was also observed in Ref. 8. In Ref. 7, a low-angle Bragg reflection was attributed to the presence of some disconnected grains of material which are not available for intercalation. However, in comparison to our data, we believe that this reflection is the result of a residue of phase I.

All three phases of $Li_xMn_2O_4$ spinel observed in this study have the same cubic structure. The only distinguishable feature is the difference in lattice constant, which was observed through the peak separation in XRD spectra. However, the lattice constants of phases I and II also change during charge-discharge, which makes it difficult to identify the phase transitions. From Fig. 1 and 3, we see the important effect of charge rate. When a high charge rate was used, the nonequilibrium state of the system increased the lattice constant ranges of phase I and phase II and resulted in the spectra in Fig. 1, which looks like a continuous lattice constant change with just one phase. When a slower charge rate was used, the spectra in Fig. 3 show clear peak separations. Because the lattice constant of phase III is almost fixed, the phase transition from phase II to phase III is easier to observe. On the other hand, the overlapping of lattice constant ranges of phase I and phase II during fast charge-discharge make it difficult to distinguish them from each other. The effect of charge rate on the nonequilibrium states is one of the important results from this study.

Conclusion

Based on in situ XRD spectra at different charge and discharge rates, a three-phase model is proposed for lithium-rich $Li_xMn_2O_4$ spinels as an intrinsic feature during lithium intercalation (deintercalation). The phase diagram based on the charging curve matched well with the phase transition observed through the XRD spectra. The charge-discharge rate has significant effects on the XRD spectra during charge-discharge.

Acknowledgment

This work was supported by the U.S. Department of Energy Division of Materials Science of the Office of Basic Energy Sciences, and the Office of Energy Research, Laboratory Technology Research Program, under contract no. DE-AC02-98CH10886.

Brookhaven National Laboratory assisted in meeting the publication costs of this article.

References

1. J. M. Tarascon, F. Coowar, G. Amatucci, F. K. Shokoohi, and D. G. Guyomard, *J. Power Sources*, **54**, 103 (1995).
2. S. Bach, M. Henry, N. Baffier, and F. K. Shokoohi, *J. Solid State Chem.*, **88**, 325 (1990).
3. P. Barboux, J. M. Tarascon, and F. K. Shokoohi, *J. Solid State Chem.*, **94**, 185 (1991).
4. T. Ohzuku, M. Kitagawa, and T. Hirai, *J. Electrochem. Soc.*, **137**, 769 (1990).
5. Y. Xia and M. Yoshio, *J. Electrochem. Soc.*, **143**, 825 (1996).
6. Y. Xia, Y. Zhou, and M. Yoshio, *J. Electrochem. Soc.*, **144**, 2593 (1997).
7. M. N. Richard, I. Keotschau, and J. R. Dahn, *J. Electrochem. Soc.*, **144**, 554 (1997).
8. W. Liu, K. Kowal, and G. C. Farrington, *J. Electrochem. Soc.*, **145**, 459 (1998).
9. S. Mukerjee, T. R. Thurston, N. M. Jisrawi, X. Q. Yang, J. McBreen, M. L. Daroux, and X. K. Xing, *J. Electrochem. Soc.*, **145**, 466 (1998).
10. J. M. Tarascon, W. R. McKinnon, F. Coowar, T. N. Bowmer, G. Amatucci, and D. Guyomard, *J. Electrochem. Soc.*, **141**, 1421 (1994).